



Title	Microcomputer Assisted Two Dimensional ESR Imaging
Author(s)	Ohno, Keiichi
Citation	Memoirs of the Faculty of Engineering, Hokkaido University, 16(3), 203-207
Issue Date	1984-12
Doc URL	<a href="http://hdl.handle.net/2115/38013">http://hdl.handle.net/2115/38013</a>
Type	bulletin (article)
File Information	16(3)_203-208.pdf



[Instructions for use](#)

# Microcomputer Assisted Two Dimensional ESR Imaging

Keiichi OHNO\*

(Received June 30, 1984)

## Abstract

The development and testing of a useful two dimensional ESR imaging system is described. A commercial 16 bit microcomputer and other associated facilities are used, which eliminate the necessity of utilization of large computers.

This system permits online operation and the realization of sufficient precision to measure spatial distributions of paramagnetic species.

## 1. Introduction

Information regarding the spatial distributions of paramagnetic species is very important for studies on transport phenomena in solid and liquid films, biological systems, chemical reactions, surface diffusion etc..

For these purposes, ESR imaging has been developed by several workers during the last five years or so<sup>1-6)</sup>. To this extent no convenient two dimensional (2D) ESR imaging has been realized for practical usages. Hoch and Day reported the first observation of 2D ESR imaging regarding the spatial distribution of paramagnetic nitrogen centers in a diamond. However they performed data processings using a large scaled off-line IBM 370/158 computer and a Surface II Graphics System. A 20 x 20 grid used was insufficient for precision.

From recent developments in microelectronics an excellent prognosis and prominent changes are predicted in the future. In the present paper a successful construction of a convenient and more precise microcomputer assisted 2D ESR imaging system will be described.

## 2. Experimental

An ESR spectrometer (JEOL FE-3XG) was modified for this purpose with an anti-Helmholtz coil pair, an available 16 bit microcomputer (NEC PC 9801) and other associated facilities.

The coil pair was attached to both outside of a universal cavity (JEOL ES-UCX2) at a distance of 45 mm and was fed pulsed DC current from two regulated programmable DC power supplies (KIKUSUI PAE 35-30) with fast transient response of 200  $\mu$ sec. The coil was made of 65 turns of copper wire (diameter 0.7 mm) with a diameter of 50 mm and provided a maximum magnetic field gradient up to 350 gauss/cm. However, a magnetic field gradient of 90 gauss/cm was used throughout this work.

The sweep of static magnetic field was controlled by the computer through a DA con-

---

\* Department of Chemical Process Engineering

verter generating pulses to drive a pulse motor. Response and convoluted spectra were digitized into 256 points per spectrum through a AD converter.

All spectra stored in RAM memories of the computer were integrated. The response spectrum was transformed into frequency domain by the fast Fourier transform (FFT) and an inverse filter function was determined by use of  $\gamma$  and  $\epsilon$  with the aid of results of the previous author's work<sup>6,7</sup>.

After the determination of the inverse filter function, each convoluted spectrum was deconvoluted to obtain a spin density projection function. Finally the reconstruction process was performed with the theory of the convolution filtering back-projection method<sup>9</sup>.

According to the theory, we have filtered profiles  $p^*$

$$p^*(r_i) = \frac{p(r_i)}{4w} - \frac{1}{\pi^2 w} \sum_{j=1, \text{ odd}}^n \frac{p(r_j)}{(i-j)^2} \quad (1)$$

where  $p(r_i)$  is the projection,  $w$  the spacing ( $=1/2 k_m$ ) and  $k_m$  the maximum spatial frequency present in image.

In practice,  $p(r_i)$ 's are observed at different angles. After the filtering we also have  $f(x, y)$ ,

$$f(x, y) = \sum_{j=1}^m p^*(x \cos \phi_j + y \sin \phi_j, \phi_j) \Delta \phi$$

where  $m$  is the number of projections and  $\Delta \phi$  is the interval between projections. A 65 x 65 grid was used for the back-projection of 36 integrated spectra observed at orientations in the range  $0^\circ$  to  $180^\circ$  every  $5^\circ$ .

Figure 1 shows a flow chart of programs used for controlling the ESR apparatus, the data acquisition, the deconvolution and the image reconstruction. All programs were compiled with the BASIC language using less than 384 kbytes memories, whereas the FFT program was compiled with a machine language.

Performance times were a few hours for total data acquisition, about 40 min for the image reconstruction, and finally about 20 min for plotting an image on the xy-plotter. However if all the programs are compiled with machine language the performance times will be greatly reduced to about one tenth of the present one.

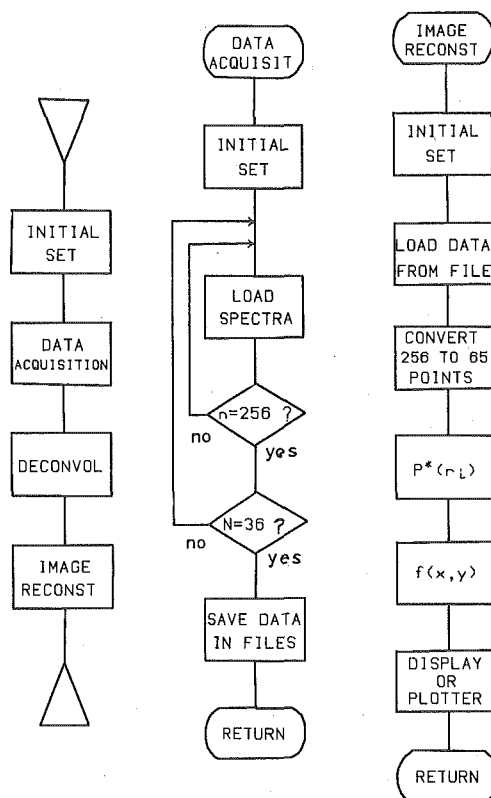


Fig. 1 Flow chart of programs for controlling ESR apparatus, data acquisition, deconvolution and image reconstruction.

## 3. Results and discussion

Two fine stable radical diphenylpicorylhydrazyl (DPPH) particles were fixed to both outside surfaces of a quartz tube (diameter 3 mm, namely the distance was 3 mm) as shown in Fig. 2. These amorphous particles have no anisotropy in ESR spectrum explicitly, the linewidth of which is a few gauss.

Thus we need not worry about the shift of the resonance line due to the anisotropy when the sample is rotated. Fig. 3 (a) shows the response function observed without magnetic field gradient.

Thirty six spectra were also observed per an image by rotating the sample every  $5^\circ$ .

Fig. 3 (b) and 3 (c) show a convoluted and a deconvoluted spectra with  $\gamma=50$  and  $\epsilon=1.1$  respectively. In order to examine the influence of  $\gamma$  and  $\epsilon$  upon images, reconstructed 2D images of DPPH solids were illustrated with various  $\gamma$  and  $\epsilon$  as shown in Fig. 4. Two peaks correspond to each DPPH solid particles and the peak heights are proportional to the quantities of paramagnetic species in the particles. The distance between them is 3 mm. Radiating lines are inevitable artifacts for the back-projection method. As a whole, the

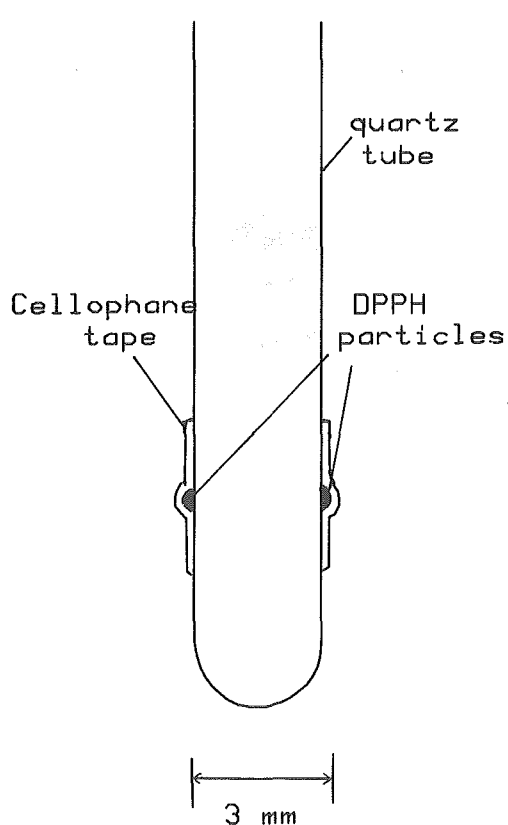


**Fig. 2** Schematic of a preliminary sample with two DPPH fine solid particles.

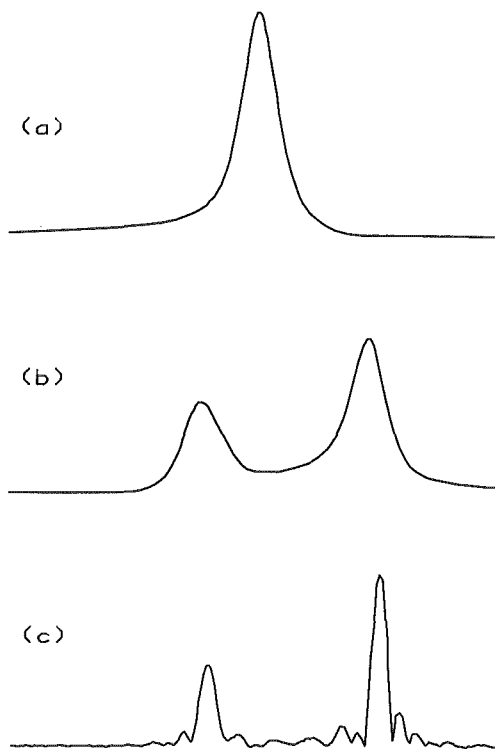


**Fig. 3** Deconvolution for ESR spectra of DPPH. (a) response function ; (b) convoluted spectrum ; (c) deconvoluted spectrum.

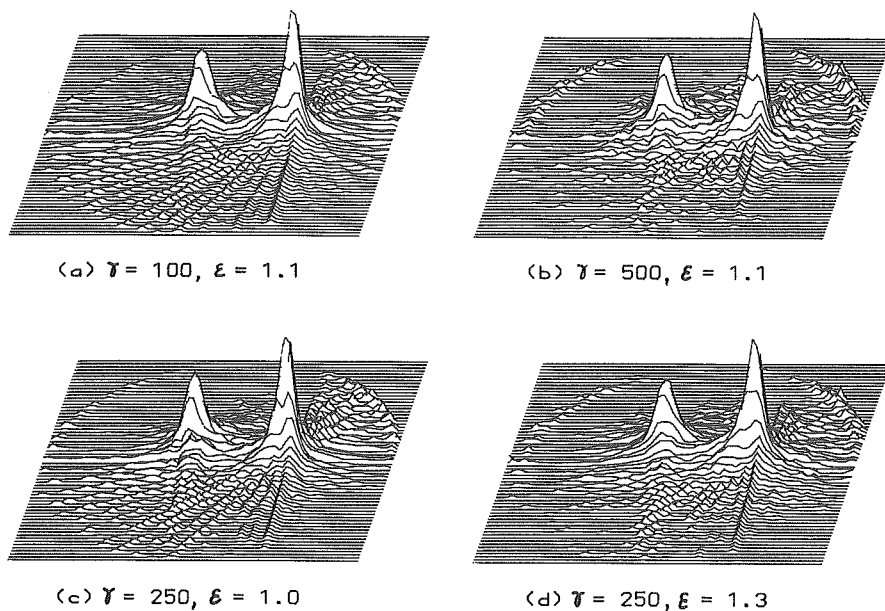


**Fig. 4** Reconstructed images from thirty six projection spectra with various  $\gamma$  and  $\epsilon$ .

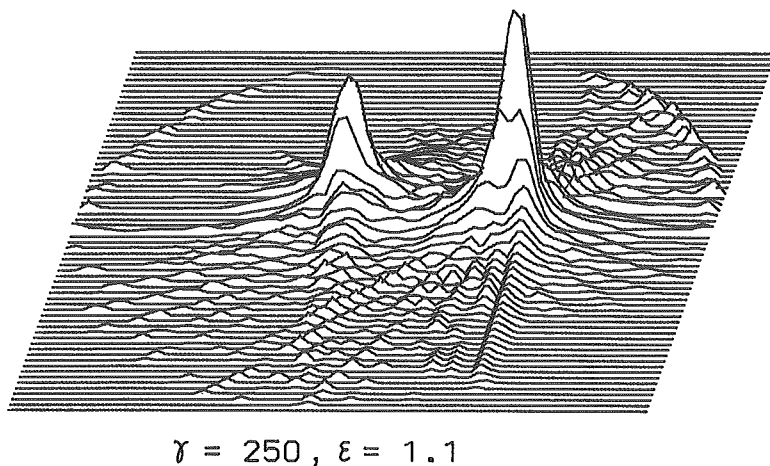


**Fig. 5** Best ESR image with  $\gamma=250$  and  $\epsilon=1.1$ .

artifacts became more remarkable as  $\gamma$  decreased, while they disappeared as  $\epsilon$  increased.

The best image was obtained with  $\gamma=250$  and  $\epsilon=1.1$  as shown in Fig. 5.

In summary, an extremely convenient and more precise 2D ESR imaging system could be constructed using a commercial 16 bit microcomputer.

This system also could be operated on-line with the ESR spectrometer and it permitted the realization of sufficient precision to measure paramagnetic density functions of the samples of less than a few millimeters size.

This work was supported by a Grant-in Aid for Developmental Scientific Research from the Ministry of Education, Science and Culture of Japan.

### References

- 1) Hohh, M. J. R. and Day, A. R. : Solid State Commun. 30 (1979) 211.
- 2) Hoch, M. J. R. : J. Phys. C, Solid State Phys. 14 (1981) 5659.
- 3) Karthe, W. and Wehrdorfer, E. : J. Magn. Reson. 33 (1979) 107.
- 4) Herrling, H. Klimes, N. Karthe, W. Ebert, U. and Ebert, B. : J. Magn. Reson. 49 (1982).
- 5) Ohno, K. : Jpn. J. Appl. Phys. 20 (1981) L179.
- 6) Ohno, K. : J. Magn. Reson. 49 (1982) 56.
- 7) Ohno, K. : J. Magn. Reson. 50 (1982) 145.
- 8) Ohno, K. : Jpn. J. Appl. Phys. 23 (1984) L224.
- 9) Brooks, R. A. and Chiro, G. Di. : Phys. Mod. Biol. 21 (1976) 689.